UNIVERSITY OF OKLAHOMA

GRADUATE COLLEGE

EVOLUTION OF OBSERVED CLOUD ORGANIZATION WITHIN TROPICAL RAINFALL EVENTS DURING THE DYNAMO/AMIE FIELD CAMPAIGN

A THESIS

SUBMITTED TO THE GRADUATE FACULTY

in partial fulfillment of the requirements for the

Degree of

MASTER OF SCIENCE

By

THERESA LINCHECK
Norman, Oklahoma
2024

Downloaded from SHAREOK. Persistent Handle URL: https://hdl.handle.net/11244/340509

EVOLUTION OF OBSERVED CLOUD ORGANIZATION WITHIN TROPICAL RAINFALL EVENTS DURING THE DYNAMO/AMIE FIELD CAMPAIGN

A THESIS APPROVED FOR THE
SCHOOL OF METEOROLOGY

BY THE COMMITTEE CONSISTING OF

Dr. Naoko Sakaeda, Chair

Dr. Kathy Pegion

Dr. Cameron Homeyer

© Copyright by THERESA LINCHECK 2024
All Rights Reserved.

Acknowledgments

I would like to acknowledge my mentors past and present for their careful guidance, wisdom, and utmost kindness in teaching me all that I know. I would also like to acknowledge my family and loved ones, who with their endless support and encouragement, helped this project come to fruition.

Table of Contents

Acknowledgments **iv**

List Of Figures **vi**

Abstract **viii**

1 Introduction **1**

2 Data & Methods **4**
2.1 DYNAMO/AMIE Field Campaign Radar Data 4
2.1.1 S-PolKa Rain Rates and Rain Type Classification 5
2.2 Cloud Organization Indices 5
2.2.1 Simple Cloud Aggregation Index (SCAI) 6
2.2.2 Morphological Index of Convective Aggregation (MICA) 7
2.2.3 Organization Index (I_{org}) 7
2.2.4 Convective Organization Potential (COP) 8
2.2.5 Radar Organization Metric (ROME) 9
2.3 Observed Convective Organization in Rainfall 10
2.3.1 Regression Analysis 10
2.3.2 Identification of Rainfall Events 11

3 Evolution of Cloud Organization in Observed Rainfall Events **12**
3.1 Evolution of Cloud Organization Indices 12

4 Evolution of Convective Organization in Rainfall Events of Differing Intensity **25**
4.1 Dependence of Cloud Organization on Intensity and Duration of Rainfall Events 25
4.1.1 Separation of Rainfall Events 25
4.1.2 Cloud Organization in Tercile Separated Rainfall Events 28

5 Summary and Conclusions **36**

Reference List **40**

List Of Figures

3.1 Time series of (a) domain mean rain rates [mm/hr], (b) I_{org}, (c) SCAI, (d) MICA, (e) COP, and (f) ROME that are reconstructed using linear time lag regression of those quantities onto the domain mean rain rate between -24hr $< \tau <$ 24hr peak rainfall events during the DYNAMO/AMIE 3-month period. The standard deviation of the domain mean rain rate was used to reconstruct all time series. Shading represents confidence intervals at the 95% level. 14

3.2 Time series of (a) domain mean rain rates [mm/hr], (b) I_{org}, (c) SCAI, (d) MICA, (e) COP, and (f) ROME for deep convective rain clusters. Time series are reconstructed using linear time lag regression of those quantities onto the domain mean rain rate of deep convective rain clusters between -24hr$< \tau <$ 24hr peak rainfall events during the DYNAMO/AMIE 3-month period. The standard deviation of the domain mean rain rate of deep convective rain clusters was used to reconstruct all time series. Shading represents confidence intervals at the 95% level 15

3.3 Time series of number N of clusters, geometric mean distance of clusters D, cluster density within rainy region (S_{cls}/A_{cls}), clear sky area fraction, mean area of clusters, spread in object cluster size Δ_{size}, and spread in object cluster proximity Δ_{prox} for all rain clusters (a, c, e, g, i, k, m) and deep rain clusters (b, d, f, h, j, l, n). Shaded regions represent confidence intervals at the 95% level. 19

3.4 A simplified schematic of the evolution of rainfall events. Light blue shaded regions indicate contiguous rain clusters and dark blue shaded regions indicate deep convective rain clusters. From (a) to (b), the number of rain clusters decrease, with remaining clusters growing in proximity and size. In the transition from (b) to (c), remaining rain clusters merge together to form a large stratiform region. Deep rain clusters decrease in size while increasing in proximity and number. . . . 24

4.1 Rainfall event composites for the lower tercile (N=15, blue), middle tercile (N=14, grey), and upper tercile (N=15,black). Composites are lagged from τ=-24hrs to τ=+24hrs. 26

4.2 Rain rate composites for the lower tercile (a), middle tercile (b), and upper tercile (c). Each rain rate tercile composite is separated into contributions from deep rain clusters (black line), stratiform rain (blue line), isolated rain clusters (yellow), and uncertain (grey line) as determined by the Powell et al. 2016. 27

4.3 Composites of domain mean rain rate (mm/hr) (a) and I_{org}, SCAI (c), MICA (d), COP (e), and ROME (f) organization indices for all rain clusters in lower (light blue), middle (blue), and upper (black) tercile separated rainfall events. Each tercile is lagged with the domain mean rain rate from τ=-24hrs to τ=+24hrs. 30
4.4 Composites of domain mean rain rate (mm/hr) (a) and I_{org}, SCAI (c), MICA (d), COP (e), and ROME (f) organization indices for deep convective rain clusters in lower (light blue), middle (blue), and upper (black) tercile separated rainfall events. Terciles are lagged with domain mean rain rate from τ=-24hrs to τ=+24hrs. 30
4.5 S-PolKa radar estimated rain rate (mm/hr) (left column) and rain type separation (right column) for an upper tercile rainfall event that occurred October 16, 2011. Scans show the progression of cloud organization from 8hrs prior to peak rain rate (row 1), time of peak rain rate (row 2), and 8hrs following peak rain rate (row 3). 32
4.6 S-PolKa radar estimated rain rate (mm/hr) (left column) and rain type separation (right column) for a lower tercile rainfall event that occurred November 16, 2011. Scans show the progression of cloud organization from 4hrs prior to peak rain rate (row 1), time of peak rain rate (row 2), and 4hrs following peak rain rate (row 3). 33

Abstract

Tropical convective organization is important for the modulation of the climate on a range of spatial-temporal scales, however the physical processes controlling organization in the atmosphere are still not fully understood. The transient nature of observed convective organization presents challenges to being accurately replicated in models, and a limited number of available observations further challenge our understanding of their driving processes. Cloud organization indices allow us to capture the evolution of cloud organization processes, however results are often sensitive to the choice in existing index used. This project aims to use cloud organization metrics to better understand how convection organizes within rainfall events observed from S-PolKa radar during the DYNAMO/AMIE field campaign. Results show that convection is most organized after peak rainfall. However, the exact timing of greatest cloud organization depends highly on the choice of indices applied. This suggests organization does not lead to increased rainfall, but rather other factors are responsible for upscale growth of tropical convection. It is also found that convective organization of rainfall events depends on the intensity of rainfall, following a sequential process from development to peak rainfall and finally decay.

Chapter 1

Introduction

Cloud organization occurs when clouds cluster together to form a larger convective cloud system that is often associated with high-impact weather events. Resulting organized cloud formations, such as mesoscale convective systems (MCSs), tropical cyclones (TCs), and aggregated cloud clusters, have large and widespread impacts on the atmosphere. For example, tropical mesoscale convection contributes over half of the precipitation in the tropics (Nesbitt et al. 2006). Organized convection also impacts the large-scale dynamics of the atmosphere by modulating the vertical diabatic heating profile, which in turn influences the Hadley and Walker circulations (Hartmann et al. 1984). Understanding how mesoscale convection organizes is therefore important for predicting large-scale climate variability, (Sakaeda and Torri 2022) which Global Climate Models (GCMs) struggle to accurately represent (Cheng et al. 2018; Cheng et al. 2020). Most GCMs are unable to resolve mesoscale organized convection due to a lack of full understanding of the processes responsible for it (Mapes and Neale 2011). More observational studies are therefore needed to elucidate how tropical organized convection evolves and improve our understanding of the physical processes that drive it.

One difficulty that quickly arises in understanding convective organization processes is that there is not a universal definition of cloud organization (Biagioli and Tompkins 2023; Sakaeda and Torri 2022). Rather, several studies have been conducted in recent years to quantify the degree of organization through the creation of cloud organization

indices. These organization metrics, designed to bridge gaps between the representation and agreement of cloud organization in models and observations, are one step towards helping achieve a more coherent definition of cloud organization. For instance, the Simple Cloud Aggregation Index (SCAI) is an organization index introduced by Tobin et al. 2012 to provide a simple diagnostic for the amount of convective aggregation present at any given time in satellite datasets and reanalyses. The Morphological Index of Convective Aggregation (MICA, Kadoya and Masunaga 2018) is another created for similar purposes of capturing self-aggregation of observed convection.

A comparison of existing cloud organization indices quickly reveals that their definitions depend on different cloud properties and variables to quantify the degree of organization, making their accuracy and applicability between different datasets and with varying spatial resolutions questionable. Some indices even seemingly contradict their own definitions of organization under certain contexts. For example, in a study published by Sakaeda and Torri 2022, it was noted that SCAI indicated the greatest degree of convective aggregation during the suppressed phase of the Madden Julian Oscillation (MJO) when there are fewer clouds present. Yet, they also pointed out that cloud organization is typically more organized during the MJO enhanced phase when larger convective systems are present, which are arguably analogous versions of real life convective aggregation. These two viewpoints demonstrate the challenges that exist when attempting to define cloud organization by a single metric. While SCAI defines "organization" as analogous to self-aggregation found in idealized models (i.e. where clouds spontaneously merge into a larger system of lesser clusters (Wing and Emanuel 2014), larger convective systems present in the MJO enhanced phase also objectively represent a valid form of greater "organization" despite the greater number of cloud clusters.

Despite differences between underlying definitions of cloud organization indices, they can still serve as a useful tool to gain a better understanding of the evolution of convective organization. For instance, Cheng et al. 2018 successfully utilized both SCAI and the simple Organization Index (I_{org}, Tompkins and Semie 2017) indices to uncover patterns of organization present within 2-day MCS events that occurred thoughout the Dynamics of the MJO/ ARM MJO Investigation Experiment (DYNAMO/AMIE) field campaign. Other studies have used cloud organization indices to discover deficiencies in model representations of convection compared to observations (White et al. 2018). This project aims to apply existing cloud organization indices to tropical convective rainfall in order to 1) better understand how organization evolves surrounding observed tropical rainfall events and 2) learn how well existing cloud organization indices capture the evolution of cloud organization associated rainfall. To that end, this project will answer the following questions:

- How do existing cloud organization indices capture the evolution of convective organization in observed rainfall events during DYNAMO/AMIE?
- How does the evolution of tropical convective organization depend on the intensity and duration of rainfall events?

This study will answer these questions by comparing how five existing organization indices capture convective organization throughout the evolution of observed rainfall events. Results will also evaluate the efficacy of each index to accurately explain peak organization during typical rainfall events. Identifying which indices are best suited for measuring organization in rainfall events will help us improve our understanding of the physical processes driving tropical organization, and help guide developments in the representation of rainfall events in models for weather and climate predictions.

Chapter 2

Data & Methods

2.1 DYNAMO/AMIE Field Campaign Radar Data

The Dynamics of the Madden Julian Oscillation/ Atmospheric Radiation Measurement Investigation Experiment (DYNAMO/AMIE) field campaign took place from 1 October 2011 - 15 January 2012 over the Indian Ocean with goals to better understand the interactions between convective clouds and the large-scale circulation of the Madden Julian Oscillation (MJO) (Zuluaga and Houze 2013). Conducted over a 4-month period, this experiment captured detailed observations of the life cycles of convective systems throughout multiple occurrences of the MJO, making it ideal to study the evolution of cloud organization. Primary data for this project is sourced from the S-PolKa dual-wavelength dual-polarized radar that was stationed on the island of Hithadoo in the Addu Atoll, Maldives (0.63°S and 73°E) (Zuluaga and Houze 2013). When deployed, S-PolKa recorded continuous dual-polarization surveillance scans (SUR) of the atmosphere at S and Ka-bands covering a 360° azimuthal area out to a 150km radius (Yoneyama et al. 2013). Resulting radar data are gridded to 1km horizontal and 0.5km vertical resolution with 15-min intervals and provide a detailed record of the evolution of the convective cloud field over the Indian Ocean within Madden Julian Oscillation (MJO) envelopes (Zuluaga and Houze 2013). S-PolKa derived data used in this project include estimated rain rates and convective types. Additional information regarding S-PolKa and the DYNAMO/AMIE campaign can be found in Yoneyama et al. (2013).

2.1.1 S-PolKa Rain Rates and Rain Type Classification

Near-surface rain rates are derived using a tropical, blended algorithm developed by Thompson et al. (2018) that relates radar reflectivity (Z) to rain rate (R). This Z-R relationship is used to determine initial rain rates, then additional relationships between differential reflectivity (Z_{dr}) and rain and specific differential phase (K_{dr}) and rain are applied to determine final rain rates (Rutledge et al. 2012). This algorithm ensures the best estimates are retrieved from S-PolKa radar during the DYNAMO/AMIE campaign. The radar-derived rain rates from S-PolKa used in this study can be found on the DYNAMO legacy website (`https://orca.atmos.washington.edu/dynamo_legacy/`)

Convective rain types are also determined from S-PolKa reflectivity data using an algorithm developed in Powell et al. (2016). This algorithm was designed to better capture weak shallow convection characteristic of the equatorial Indian ocean. It takes 1 km x- and y-gridded S-PolKa radar reflectivity data and converts it to one of several convective rain types - stratiform, convective, mixed, isolated convective core (ICF), isolated fringe (ICF), and weak echo. Further information on the details of this algorithm can be found on the DYNAMO legacy website previously mentioned. Using this algorithm, a "rain cluster" in this study is defined as a contiguous area of rain of any rain type which includes all the listed categories above. A "deep convective rain cluster" is defined as a contiguous area of the convective rain type.

2.2 Cloud Organization Indices

Five cloud organization indices are calculated and compared throughout this study to gain a better understanding of how convection organizes in tropical rainfall events during DYNAMO/AMIE. The cloud organization indices introduced below are calculated as in Sakaeda and Torri (2022) by determining the number of rain clusters,

horizontal sizes, and distances between each pair of rain clusters at each 15-min radar volume scan. Rain clusters are defined in this study as contiguous areas of nonzero near-surface rain rate from all rain types included in the Powell et al. (2016) algorithm. Cloud organization indices are also calculated for deep convective rain clusters, which are defined as contiguous areas of nonzero convective rain type.

2.2.1 Simple Cloud Aggregation Index (SCAI)

Aggregation is a state of cloud organization often seen in idealized convection that occurs when clouds organize to have a smaller number of larger convective systems (Sakaeda and Torri 2022). The Simple Cloud Aggregation Index (SCAI, Tobin et al. 2012) measures the degree to which a convective system is aggregated. Defined as:

$$SCAI = 1000 \times \frac{N}{N_{max}} \frac{D}{L} \tag{2.1}$$

SCAI compares the number N of cloud or rain clusters to the number N_{max} of maximum potential clusters, defined as half the total number of grid points, that occur in a characteristic domain of length L. D is defined as the geometric mean distance between cluster centroids of all cluster pairs in the domain. A smaller SCAI value indicates greater aggregation as the number N of clusters decreases, while a larger SCAI value indicates less aggregation. SCAI is therefore strongly dependent on N.

2.2.2 Morphological Index of Convective Aggregation (MICA)

Similar to SCAI, the Morphological Index of Convective Aggregation (MICA, Kadoya and Masunaga 2018) measures how aggregated convection within a domain is by considering the concentration of cloud clusters. MICA is defined as

$$MICA = \frac{\sum_{i=1}^{N} S_{cls,i}}{A_{cls}} \frac{(A_{obs} - A_{cls})}{A_{obs}} \tag{2.2}$$

where $S_{cls,i}$ is the area of the i^{th} cluster, A_{cls} is the area of the smallest possible rectangle enclosing all clusters or cloud objects in the domain, and A_{obs} is the total observed domain area. The first fraction ($\frac{\sum_{i=1}^{N} S_{cls,i}}{A_{cls}}$) calculates the density of clusters within the cloudy region (Sakaeda and Torri 2022), and the second fraction ($\frac{(A_{obs}-A_{cls})}{A_{obs}}$) calculates the clear sky area fraction within the domain. The value of MICA increases as clusters become more concentrated in one part of the domain. While MICA accounts for more parameters in diagnosing regions of self-aggregation, domains that include outliers far from the primary aggregates or have broadly scattered objects such as tropical synoptic organization can reduce the accuracy of MICA (Biagioli and Tompkins 2023). To apply MICA to S-PolKa radar data in this project, area A_{cls} is defined as the smallest possible circle enclosing all clusters.

2.2.3 Organization Index (I_{org})

Another way to define cloud organization is to categorize its state as either random, clustered ("non-random"), or regular (Biagioli and Tompkins 2023). The organization index (I_{org}, Tompkins and Semie 2017) diagnoses the degree of non-randomness by calculating the nearest neighbor distances (NNDs) between cloud clusters and comparing the cumulative distribution of nearest-neighbor distances (NNCDF) in that domain. Mathematically, I_{org} is defined as

$$I_{org} = \sum NNCDF(d)\,[NNCDF_{random}(d + \delta d/2) - NNCDF_{random}(d - \delta d/2)] \quad (2.3)$$

where d is the distance measured between nearest-neighbor cluster centroids, and $NNCDF_{random}$ is the cumulative distribution of randomly distributed clusters, defined as

$$NNCDF_{random}(d) = 1 - exp(-\lambda \pi d^2) \quad (2.4)$$

In simple terms, I_{org} is a ratio between the actual NNCDF and random NNCDF. If both terms are the same, I_{org} is equal to 0.5 and the organization is considered to be randomly distributed. I_{org} measures how much the cloud organization deviates from the random distribution. If clusters are closer together than when randomly distributed (Sakaeda and Torri 2022), the value of $I_{org} > 0.5$ and clusters are considered clustered or non-random. A regular distribution corresponds to $I_{org} < 0.5$ and occurs when clusters are further apart on average than expected from a random distribution (Tompkins and Semie 2017). This index does not consider the size of objects. Rather, Equation 2.3 shows the expected random distribution of points, which does not necessarily account for observed clusters with nonzero size.

2.2.4 Convective Organization Potential (COP)

The Convective Organization Potential (COP, White et al. 2018) diagnoses "clustering" in a cloud field by considering the total number N of objects in a scene, the size (area)

of the objects, and the distance between the objects. This results in an "organization potential" for any given cloud field which is defined as

$$COP = \frac{\sum_{i=1}^{N} \sum_{j=i+1}^{N} V(i,j)}{(1/2)N(N-1)} \tag{2.5}$$

where

$$V(i,j) = \frac{\sqrt{A_i} + \sqrt{A_j}}{d(i,j)\sqrt{\pi}} = \frac{r_i + r_j}{d(i,j)} \tag{2.6}$$

$V(i,j)$ is a dimensionless interaction potential calculated between every pair of objects where A_i and A_j are the object areas, $d(i,j)$ is the distance between object centroids, and r_i, r_j are the object radii. $V(i,j)$ increases when r_i, r_j increase or $d(i,j)$ decrease, considering both the size and proximity of two object clusters to interact. For N objects, COP is therefore a sum of all the interaction potentials divided by the total number of connections between objects (White et al. 2018). Objects that are larger and closer together (i.e. more "clustered") have greater COP values, while scenes with objects that are smaller and farther apart have smaller COP values.

2.2.5 Radar Organization Metric (ROME)

Finally, the Radar Organization Metric (ROME, Retsch et al. 2020) is an organization metric based on tropical radar observations that considers the size and proximity of convective regions. Similar to COP, ROME determines all unique connections between object pairs (Retsch et al. 2020) and assigns a scalar value c to each pair before taking the mean of all c values. Here, c is defined as

$$c = A_a + min\left(1, \frac{A_b}{A_d}\right) \cdot A_b \tag{2.7}$$

which includes the area of the larger object A_a (km^2) in a pair plus the area of the smaller object A_b , multiplied by a weight A_d that is the smallest area (i.e. shortest distance squared) between both objects in the pair. For N objects in the domain, ROME is then defined as

$$ROME = \begin{cases} \frac{1}{k}\sum_{i=1}^{k} c_i, k = \frac{1}{2}N(N-1) & \text{for } N > 1 \\ A_a & \text{for } N = 1 \end{cases} \tag{2.8}$$

If only one convective object is present in the radar image, then ROME is equal to A_a. This index has a primary dependence on size, proximity, and size distribution of convective elements, and can therefore also be defined as ROME = $\bar{\text{A}}$ + Δ_{prox} + Δ_{size} (Retsch et al. 2020). Here, $\bar{\text{A}}$ is the mean size of clusters, Δ_{size} is the contribution to ROME due to the spread in object cluster sizes, and Δ_{prox} is the contribution to ROME due to the proximity of clusters. When any of these terms increases, ROME also increases.

2.3 Observed Convective Organization in Rainfall

2.3.1 Regression Analysis

A time lag regression is performed for each cloud organization index in this study to better observe the typical evolution of convective organization associated with observed rainfall during the 3-month DYNAMO period. A time lag auto regression of domain mean rain rates onto themselves is first performed from τ = -24hrs to τ = +24hrs. The rain rate time series (i.e. predictand) is then reconstructed using the standard deviation of the domain mean rain rate. Each cloud organization index is regressed onto the domain mean rain rate following the same method, reconstructing the time

series of each organization index using the standard deviation of the domain mean rain rate. The resulting reconstructed time series of organization indices encapsulate how convective organization associated with observed rainfall evolves in the 24hrs leading up to and following peak rain rate during DYNAMO.

2.3.2 Identification of Rainfall Events

To investigate how the organization and evolution of observed convection depends on rainfall intensity, rainfall events during the DYNAMO/AMIE field campaign are identified and composited into terciles according to their relative strength and duration. Events are identified using S-PolKa domain-averaged near-surface rain rate estimates. The rain rate time series is smoothed using a triangle running mean over a 6-hour window. Rainfall events are then defined as whenever a relative rain rate maximum occurs and 1) no other rain rate maxima occur within a 6-hour window or 2) the rain rate drops below 0.5mm/hr between two events. If two rain rate maxima occur within 6 hours of each other, the rainfall event is defined as the larger relative rain rate maxima. If two rain rate maxima are greater than 6 hours apart of each other and no rain rates below 0.5mm/hr occur between each other, the two rain rate maxima are considered the same rainfall event and the first maxima is defined as that event maximum.

Using the above algorithm, a total of 44 separate rainfall events are identified within the 3-month period of DYNAMO/AMIE. The 44 events are separated into 3 terciles depending on the value of the relative rain rate maximum in each event; 0 – 0.68mm/hr (lower tercile), 0.69 – 1.09mm/hr (middle tercile), and 1.1–2.5mm/hr (upper tercile). Rainfall events are then composited within each tercile according to rain rate maximum along a time lag τ of -24 to +24 hours. This compositing and analysis process can then be extended to each organization index.

Chapter 3

Evolution of Cloud Organization in Observed Rainfall Events

3.1 Evolution of Cloud Organization Indices

The objective of this chapter will be to investigate how cloud organization indices introduced in Section 2.2 capture the evolution of convection associated with observed rainfall during DYNAMO/AMIE. We will demonstrate that the time of greatest cloud organization surrounding relative rainfall maxima varies largely depending on the index used to measure the organization. We will further show that cloud organization is greatest after rainfall peak (i.e. rain rate maxima) regardless of the index used to quantify it, suggesting that convective organization does not lead to rainfall maxima. Instead, results suggest that cloud organization is a process to maintain or prolong rainfall, or a precursor to further strengthen convective organization.

The indices also demonstrate that different types of rainfall are most present during various stages of convective evolution (i.e. isolated deep convective versus broad stratiform rain). While further work is needed to improve how convective organization is objectively defined, the following results still give us important insights into how convection evolves in rainfall events and the physical drivers behind them.

Figure 3.1a shows the typical evolution of rainfall from all rain clusters beginning 24hrs leading up to and 24hrs following rainfall events during DYNAMO. It is calculated by performing a time lag auto-regression of S-PolKa estimated rain rates onto themselves, then reconstructing the time series using the standard deviation of the time and domain mean rain rate. The resulting time series in Fig. 3.1a shows the typical evolution of DYNAMO rainfall events with a timescale of approximately 2-days. A similar time lag regression is performed for deep convective rain clusters, which are rain clusters defined as "contiguous areas of nonzero near-surface S-PolKa rain rates" (Sakaeda and Torri 2022) and categorized as deep convective by the Powell et al. (2016) rain typing algorithm. The reconstructed time series for deep convective rain rates in Fig. 3.2a shows a similar evolution of rainfall as in Fig. 3.1a, but with a smaller peak rain rate at $\tau = 0$hrs. This smaller rain rate indicates that deep convection contributes a fraction of the total rainfall in DYNAMO rain events, and demonstrates that total rainfall comes from a combination of deep convective rain clusters and other types (e.g. stratiform, isolated, uncertain). In both Fig. 3.1a and Fig. 3.2a, the leading timescale of 2-days can be explained by the multiple 2-day rain episodes observed within the 3-month observational period (Zuluaga and Houze 2013; Cheng et al. 2018).

Figures 3.1 b-f show how the SCAI, I_{org}, MICA, COP, and ROME cloud organization indices typically evolve from 24hrs leading up to and 24hrs after rainfall peaks. Each organization index is calculated using rain clusters identified from estimated S-PolKa rain rates. Then as in Fig. 3.1a, a time lag regression analysis is performed for each index onto the domain mean rain rate, and a time series of each organization index is reconstructed using the standard deviation of the domain mean rain rate as the predictor. From these reconstructed timeseries, we are able to gain insight into how cloud organization evolves surrounding the time of peak rainfall.

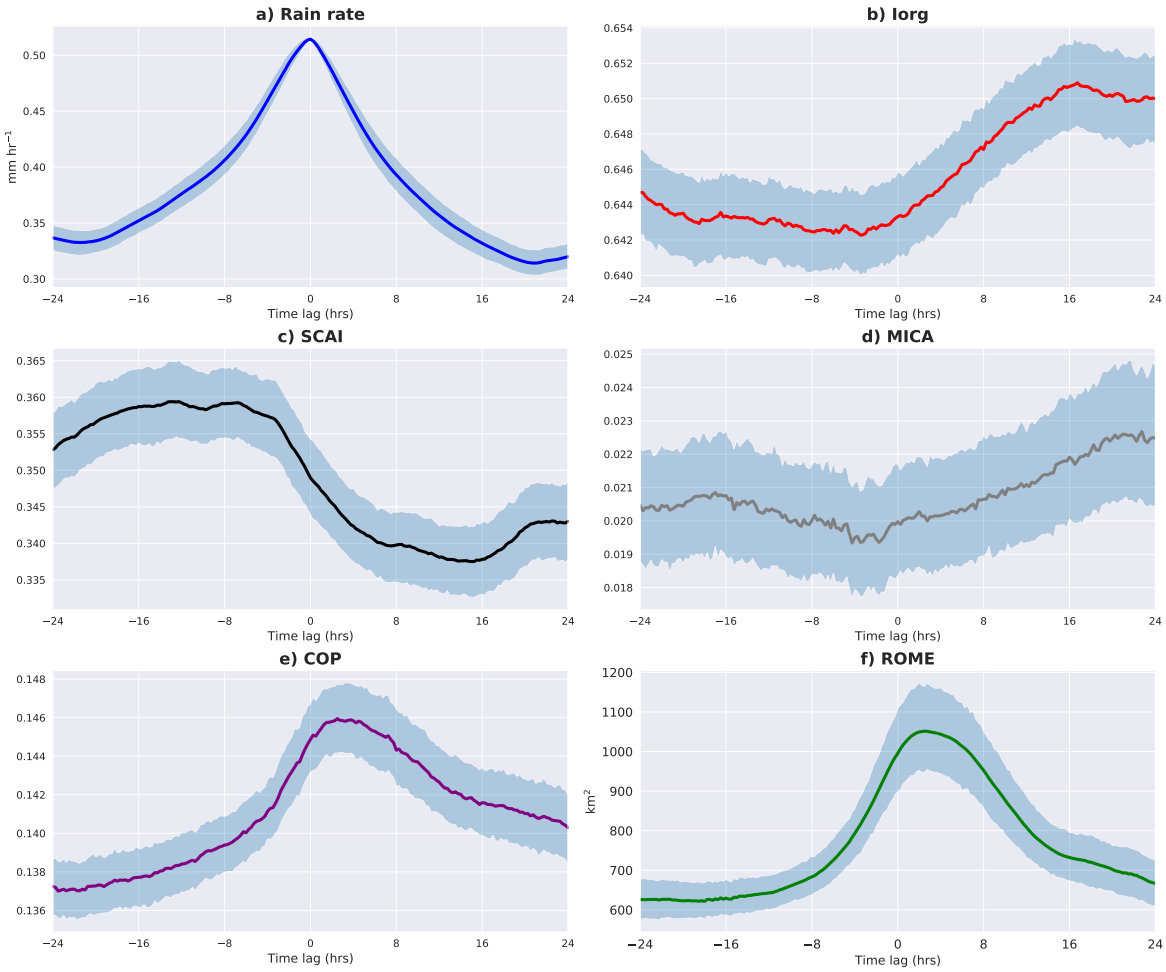


Figure 3.1: Time series of (a) domain mean rain rates [mm/hr], (b) I_{org}, (c) SCAI, (d) MICA, (e) COP, and (f) ROME that are reconstructed using linear time lag regression of those quantities onto the domain mean rain rate between -24hr $< \tau <$ 24hr peak rainfall events during the DYNAMO/AMIE 3-month period. The standard deviation of the domain mean rain rate was used to reconstruct all time series. Shading represents confidence intervals at the 95% level.

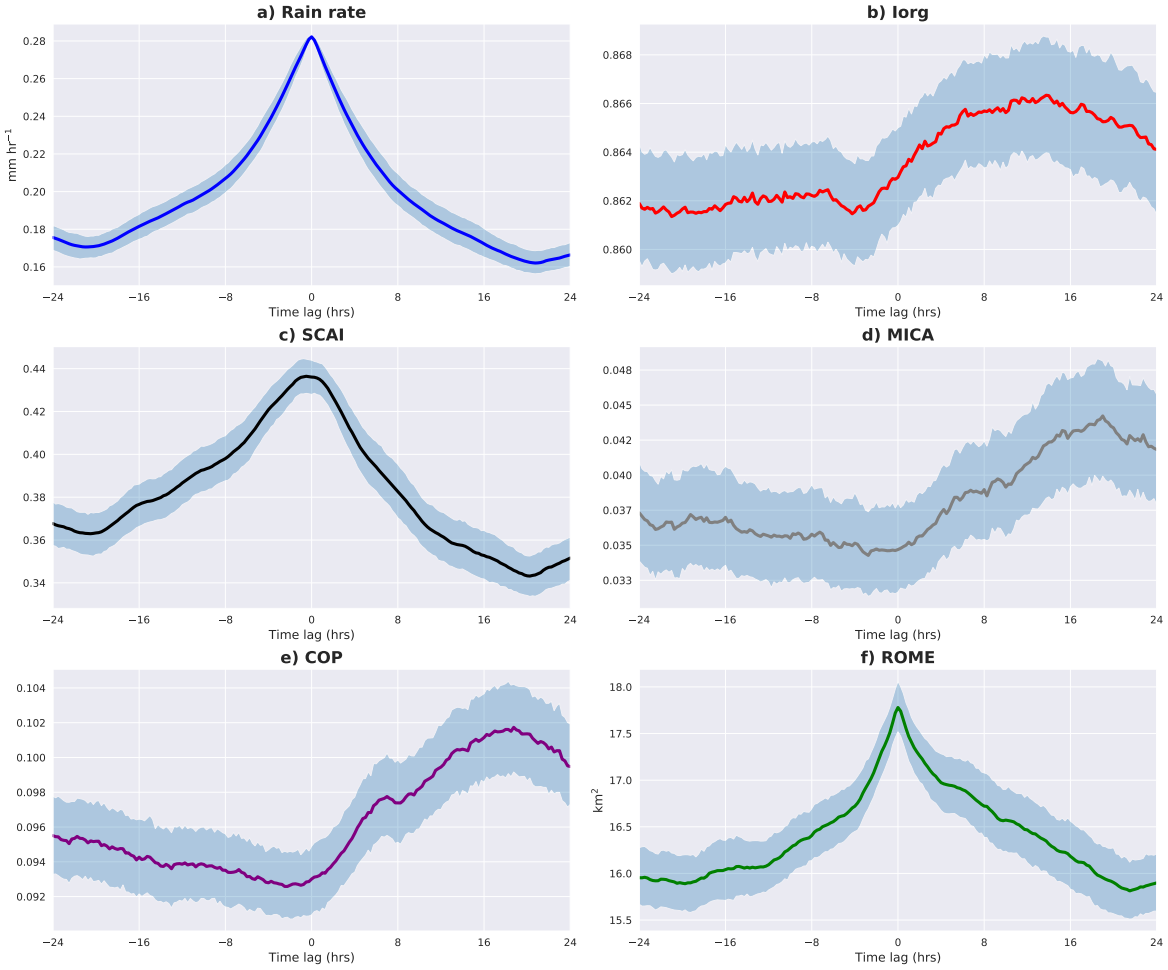


Figure 3.2: Time series of (a) domain mean rain rates [mm/hr], (b) I_{org}, (c) SCAI, (d) MICA, (e) COP, and (f) ROME for deep convective rain clusters. Time series are reconstructed using linear time lag regression of those quantities onto the domain mean rain rate of deep convective rain clusters between -24hr$< \tau <$ 24hr peak rainfall events during the DYNAMO/AMIE 3-month period. The standard deviation of the domain mean rain rate of deep convective rain clusters was used to reconstruct all time series. Shading represents confidence intervals at the 95% level

I_{org} in Fig. 3.1b shows that convection transitions from a slightly non-random state (-10hr to 0hr) before rain maxima, to an increasingly non-random state well after rain maxima (+16 hr). This result implies that convection is most non-random or organized hours after rainfall peaks and subsides in the later weakening stages of convection. While this at first appears counter-intuitive, this increase in I_{org} can be explained by a preferential formation of new clusters in close proximity to existing clusters during this decaying stage. I_{org} is dependent on nearest-neighbor distances (NND) between rain clusters (Cheng et al. 2018), therefore as the number of rain clusters with smaller NND increases in the later stages of convection, I_{org} increases as well. This I_{org} behavior is also seen in Fig. 3.2b for deep convective rain clusters, which indicates that the NND of deep convection decreases hours after rainfall has begun to subside. Compared to all rain clusters, I_{org} of deep convective rain in 3.2b peaks a few hours earlier, indicating that deep convection tends to organize earlier in the decaying stage, or stage that occurs after peak rainfall (i.e. $\tau > 0$hrs). It is important to note that I_{org} does not consider the sizes of clusters, therefore it has limitations in well representing a scene containing a large variability in cluster size (Sakaeda and Torri 2022) such as with all rain clusters in Figure 3.1b. As the size variability decreases in deep convective rain clusters in Figure 3.2b, the applicability of I_{org} becomes more appropriate.

SCAI captures how the degree of aggregation evolves leading up to and following peak rainfall for all rain clusters (Fig. 3.1c) and (Fig. 3.2c) deep convective rain clusters. In Figure 3.1c, SCAI minimizes +14hrs after rain maxima, indicating that observed aggregation is greatest well after rainfall has peaked and subsided. To understand why this is the case, we look at how the number of clusters N and geometric mean distance between cluster pairs D, which SCAI directly depends upon (Cheng et al. 2018), evolve over time. Figure 3.3a shows that the number of rain clusters N is greatest just prior to peak rain rate (-8hr to -4hr) before decreasing to a minimum around

+12hrs past peak rainfall, and is accompanied by a steady decrease in D beginning -8hr onwards (Fig. 3.3c). The decrease in N around peak rain rate reflects a decrease in the development of new rain clusters and a merging of existing systems. The accompanying decrease in D further indicates that any new convection that forms does so preferentially near already existing convection after peak rainfall. It also may reflect that any isolated rain clusters far from others are disappearing preferentially before rain clusters that are closer to one another.

This time evolution of organization supports a 2 phase process of convective clustering introduced in Cheng et al. 2018, where Phase 1 convection forms in closer proximity to existing convection (indicated by increasing N and I_{org} while D remains nearly constant) prior to peak rain rate, and Phase 2 convection promotes aggregation and maintenance of clustering (reflected by a decrease in N and D, and an increase in I_{org}). This 2 phase process of convective organization is especially prominent in Figures 3.3b,d for deep convective rain clusters, where N (and SCAI) closely follow the shape of the time evolution of the deep convective rain rate (Fig. 3.2c). Cheng et al. 2018 also observed a similar time evolution for N following the domain rain rate for 2-day rain episodes measured by S-PolKa, and suggested that N is a greater indicator of the convective rain rate rather than clustering. While the time evolution of N in Fig. 3.3b does indeed reflect the evolution of the deep convective rain rate in Fig. 3.3a, the time evolution of N for all rain clusters in Fig. 3.3a fails to also reflect the domain mean rain rate shown in Fig. 3.1a. Therefore our results show that N cannot be inferred to always reflect the mean rain rate of the observed convection. As its been observed in previous studies though (Stein et al. 2017; Cheng et al. 2018; Sakaeda and Torri 2022), SCAI closely follows the shape of N due to its large variability compared to D, and is therefore strongly dependent on N. This means that even in cases of enhanced convection where there is a high number N of clusters such as in Fig. 3.3a before peak rain rate, SCAI

will interpret the observed organization as being less aggregated, such as is the case in Fig. 3.1c before peak rain rate. The results of this study therefore show that SCAI cannot adequately represent organization occurring in DYNAMO rainfall events, and supports previous studies' conclusions that SCAI is not well suited for higher-resolution data such as S-PolKa (Cheng et al. 2018).

Similar to SCAI, MICA also measures how aggregation evolves over time within all convective rain clusters (Fig. 3.1d) and deep convective rain clusters (Fig. 3.2d) surrounding the peak rain rate. In Fig. 3.1d, a minimum in MICA occurs at -4hrs, followed by a linear increase at -2hr that continues well after rain maxima (e.g. +16hr). This indicates that rain clusters are most dis-aggregated in the immediate hours prior to peak rainfall before slowly becoming more aggregated after rainfall maximum. Results in Fig. 3.2d show a similar evolution for deep convective rain clusters with a minima occurring just before rain maxima followed by a steady increase after the deep rain rate maxima. These results imply that both all rain clusters and deep convective rain clusters evolve from their most dis-aggregated state just before peak rain rate to the most aggregated or organized state several hours after rain maximum has passed. While interpreting these results from MICA, it is important to note any limitations of the organization index. For instance, it has been previously observed that MICA tends to be dominated by the fraction of overall clear area present in the domain(Sakaeda and Torri 2022). Comparing the clear area fraction for all rain clusters (Fig. 3.3}g) and deep rain clusters (Fig. 3.3h) to MICA in Fig 3.1d and Fig. 3.2d respectively, it is apparent that MICA reflects the shape of the clear area fraction measured. This means that MICA is highly sensitive to the domain chosen to observe cloud organization. Despite this limitation, it is still possible to discern certain characteristics of the cloud organization through the cluster density term in MICA. In Fig. 3.3e, the density of

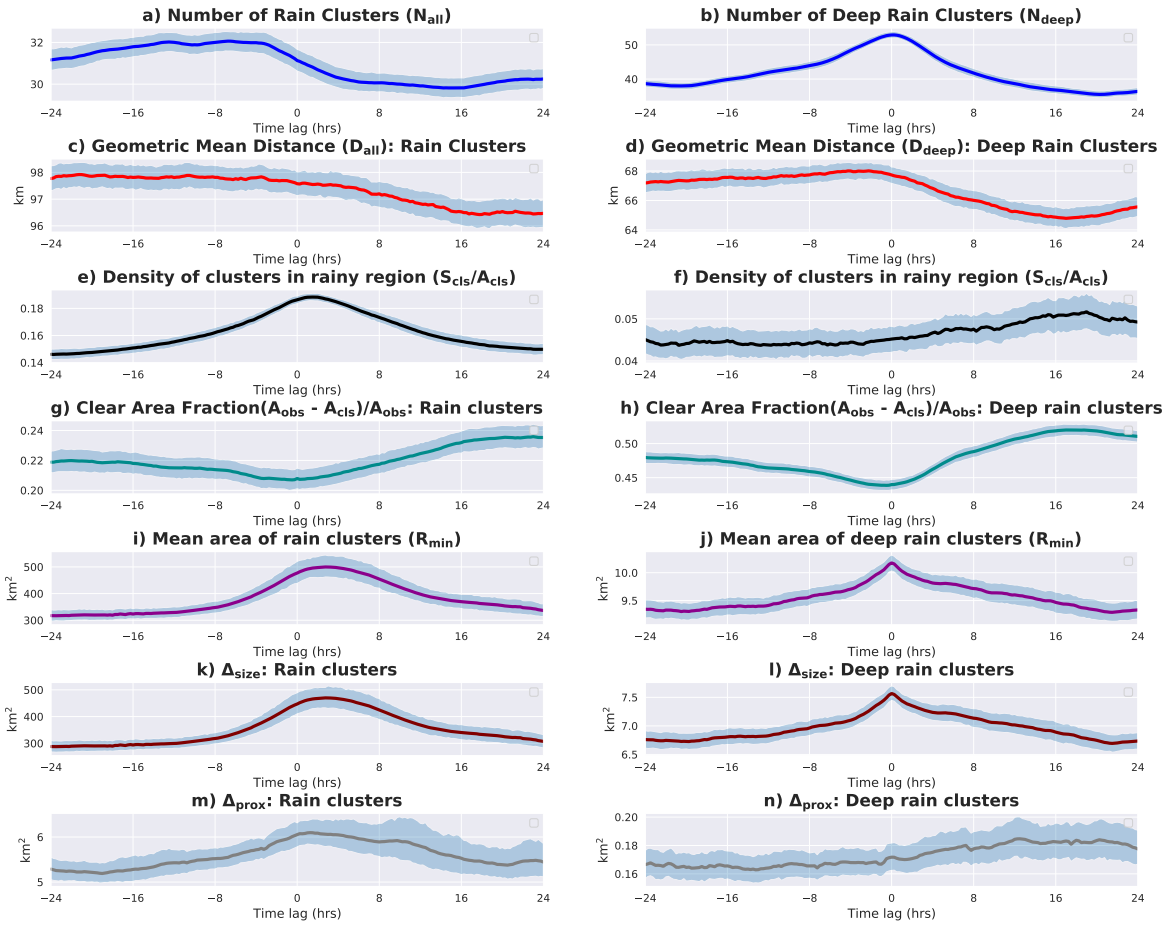


Figure 3.3: Time series of number N of clusters, geometric mean distance of clusters D, cluster density within rainy region (S_{cls}/A_{cls}), clear sky area fraction, mean area of clusters, spread in object cluster size Δ_{size}, and spread in object cluster proximity Δ_{prox} for all rain clusters (a, c, e, g, i, k, m) and deep rain clusters (b, d, f, h, j, l, n). Shaded regions represent confidence intervals at the 95% level.

rain clusters maximizes just after peak rainfall occurs before falling again as rainfall slows and convection decays. This behavior is not replicated in Fig. 3.3f for deep rain clusters. Instead, the density of clusters for deep convective clusters remains mostly constant until hours after peak rainfall has occurred, with most notable increases in density occurring +8hrs after maximum rainfall. This means that while non-deep rain clusters begin to dissipate after peak rainfall, deep convective clusters tend to remain and become more organized in the later phase of convective evolution. Overall, these results indicate that MICA can not reliably identify times of greatest apparent aggregation (i.e. low MICA at 0hrs while the density of rain clusters is maximum), and is sensitive to how clusters are defined (Sakaeda and Torri 2022).

COP considers both the size (radius) and proximity of clusters. From -8hr to maximum rainfall at 0hrs, COP (Fig. 3.1e) rapidly increases for all rain types, signaling an apparent increase in clustering organization. As this increase occurs, the mean rain cluster area also increases, shown in Fig. 3.3i. At peak rainfall to 4hrs after peak rain rate, the number of rain clusters and COP both maximize, before decreasing at +4hrs and onwards. The parallel behavior of mean cluster area and COP demonstrates that for all rain clusters, COP primarily depends on the mean cluster area. For the organization of deep convective rain clusters (Fig. 3.2e), COP shows a very different trend, with the most disorganized state occurring immediately before greatest rain rate (e.g. -2 to -1hr in Fig. 3.2e). However, the mean area of deep convective rain clusters (Fig 3.2j) is greatest at the time of maximum rain (0hr). This implies that the minima in COP (Fig. 3.2e) at 0hrs is not explained the mean size of the deep convective rain clusters here. Rather, since COP depends on both cluster size and proximity, a small COP value and large mean cluster area indicates that the proximity of deep rain clusters must be small (i.e. deep rain clusters are far apart from each other). Indeed following time after peak rain rate (0hr), COP continuously increases until +16hrs despite a

constant decrease in the mean area of deep rain clusters (Fig. 3.3j). The increase in COP after 0hrs is therefore explained by a substantial increase in the proximity of deep rain clusters (i.e. a constant decrease in the distance between clusters). In summary, COP demonstrates that prior to rain rate, deep convective rain clusters organize by increasing in size. Then after maximum rainfall, deep rain clusters continue to organize by becoming closer in proximity to each other (i.e. increased clustering).

Similar to COP, ROME determines the degree of convective organization based on the average size, proximity, and distribution of sizes of object clusters. With contributions from these components, ROME can be broken down into ROME = $\bar{A}$ + Δ_{prox} + Δ_{size} (Retsch et al. 2020) where $\bar{A}$ is the mean size of clusters. Here Δ_{size} is the contribution to ROME due to the spread in object cluster sizes and Δ_{prox} is the contribution to ROME due to the proximity of clusters. Δ_{size} increases as the spread in object cluster sizes increases, and Δ_{prox} increases as object clusters become closer together (i.e. more clustered). When applied to all rain clusters, ROME indicates little organization -8hrs prior to peak rainfall (Fig. 3.1f). This is followed by a steady increase in ROME (Fig. 3.1f) until approximately +3hrs, indicating maximum organization occurs shortly after peak rainfall. A similar trend is observed in $\bar{A}$ (i.e. R_{min}) in Fig. 3.3i and Δ_{size} in Fig. 3.3k. This shows that the increase in cloud organization by ROME coincides with an increase in the average size of rain clusters and an increase in the distribution of their sizes shortly after rainfall maxima. The Δ_{prox} (Fig. 3.3m) also contributes to ROME and captures a slow decrease in the proximity of rain clusters after rain maxima, but it is several orders of magnitude smaller than $\bar{A}$ and Δ_{size} and has much less of an impact on ROME.

ROME applied to deep rain clusters shows an earlier peak in organization, maximizing at 0hrs with peak rain rate (Fig. 3.2f). This peak coincides with maxima in both the mean area of deep rain clusters (Fig. 3.3j) and distribution of sizes Δ_{size} (Fig. 3.3l)

and again shows how they contribute to the overall shape of ROME. It is interesting to note the steady increase in proximity of deep rain clusters Δ_{prox} (Fig. 3.3n) compared to the decrease in proximity for all rain clusters (Fig. 3.3m). While a couple orders of magnitude smaller than $\bar{\text{A}}$ and Δ_{size}, Δ_{prox} captures how proximity (clustering) increases for deep rain clusters after peak rainfall in comparison to all rain clusters, which tend to decrease in proximity (become less clustered) after peak rainfall.

Overall results demonstrate that cloud organization indices disagree on the timing of greatest cloud organization surrounding rainfall maxima. This is due to each organization index relying on different parameters and physical properties within their respective definitions. For example, SCAI decreases as the number N of contiguous clusters decreases, therefore SCAI indicates the greatest degree of aggregation when the number N all rain clusters is small hours after peak rainfall. In comparison, MICA increases as the domain clear area fraction increases, therefore MICA will show the greatest aggregation when the rain clusters occupy the least amount of domain area. Other examples include COP's sensitivity to the mean size of clusters, which can make it increase if the distance between clusters decreases. ROME is mainly sensitive to the mean size of clusters. Finally, I_{org} increases as the spatial distribution of clusters becomes more concentrated in a specific region of the radar domain. Reliance on these various parameters demonstrates that certain indices will maximize before peak rainfall, while others will preferentially maximize during or after peak rainfall depending on the characteristics they depend on the most.

Despite disagreement amongst cloud organization indices, a deeper investigation of the cloud properties themselves reveals a broader pattern in which clouds typically organize and evolve surrounding maximum rainfall. This pattern, shown in Figure 3.4, is shown in three typical stages - a developing stage, peak rainfall stage, and decaying stage. In the developing stage (Fig. 3.4a), the number of all rain clusters (light blue)

is greatest, the mean size is small, and there is a wider spread in distance between clusters. Meanwhile, deep convective rain clusters (dark blue) are fairly uniform in size and small in number but still increasing with a large mean distance between them. They are also more spread out across the domain. In stage 2 (Fig. 3.4b), peak rainfall is accompanied by a decrease in non-deep convective rain clusters and increase in deep convective rain clusters. The non-deep rain clusters that remain merge closer together and grow in average size. Deep rain clusters also increase in number and size, however do not grow as clustered as non-deep convective rain. Finally, the decaying stage 3 (Fig. 3.4c) is marked by an increase in the clear area fraction but increased density of all and deep rain clusters in one spot.

This 3 stage process reinforces previous results about the development and evolution of observed MCS convection in the tropics Cheng et al. 2018. In the next section, it will be explored how rainfall event organization evolves with differing intensities and duration of rainfall, and whether this pattern persists across the full spectrum of intensities.

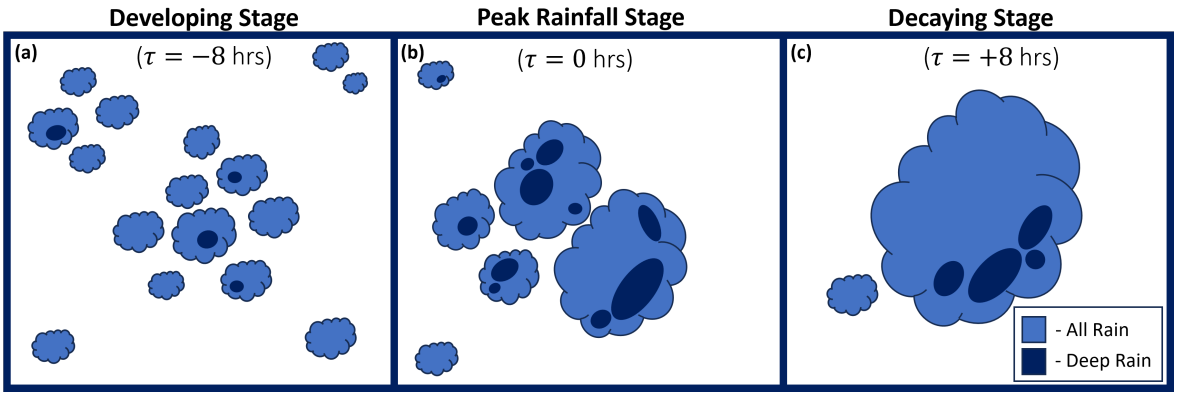


Figure 3.4: A simplified schematic of the evolution of rainfall events. Light blue shaded regions indicate contiguous rain clusters and dark blue shaded regions indicate deep convective rain clusters. From (a) to (b), the number of rain clusters decrease, with remaining clusters growing in proximity and size. In the transition from (b) to (c), remaining rain clusters merge together to form a large stratiform region. Deep rain clusters decrease in size while increasing in proximity and number.

Chapter 4

Evolution of Convective Organization in Rainfall Events of Differing Intensity

4.1 Dependence of Cloud Organization on Intensity and Duration of Rainfall Events

In the previous chapter, we found that the typical evolution of cloud organization within observed rainfall events occurs in three stages in the hours prior to, during, and after peak rainfall. Here we investigate if and how this pattern of organization persists in rain events with differing intensities (i.e. different maximum rain rates) and duration. We also investigate how the degree of organization within these events depends on the rain rate.

4.1.1 Separation of Rainfall Events

To better understand how cloud organization evolves with differing rainfall intensities (i.e. differing maximum rain rates), rainfall events that occurred during DYNAMO/AMIE are identified and sorted into terciles and composited based on the peak rain rate [mm/hr]. Following the algorithm discussed in Section 2.3.2, N = 44 separate rainfall events are identified within the three month period, with 15 events occurring in the lowest rain rate tercile, 14 in the middle tercile, and 15 in the upper

tercile. Composites of each rain rate tercile are lagged from τ=-24hrs to τ=+24hrs and shown in Figure 4.1.

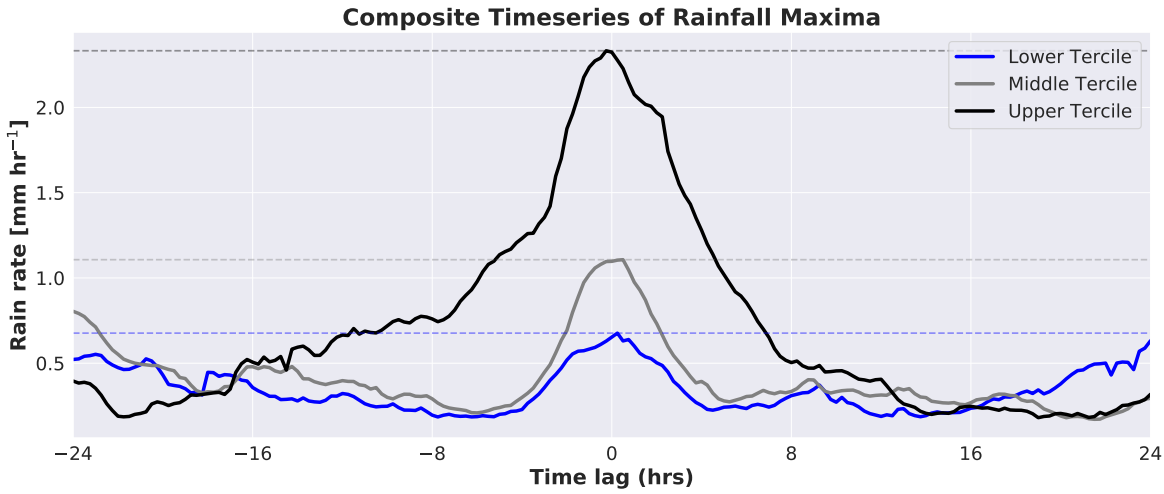


Figure 4.1: Rainfall event composites for the lower tercile (N=15, blue), middle tercile (N=14, grey), and upper tercile (N=15,black). Composites are lagged from τ=-24hrs to τ=+24hrs.

Figure 4.1 demonstrates that the majority of rainfall is contributed from upper tercile rain events, while middle and lower tercile rainfall contribute to a lesser amount and shorter duration of rainfall. Further separation of composites into their rain type components in each tercile (Fig. 4.2) shows that the majority of rainfall within each tercile comes from deep convective rain. As the intensity of rain in an event increases, the percentage of rainfall that comes from stratiform also increases. For example, the percentage of stratiform rain to deep convective rain in the lowest tercile at peak rainfall (τ = 0hrs) is approximately 14% (Fig. 4.2c). In comparison, the ratio of stratiform to deep convective rain is approximately 25% in the upper tercile (Fig. 4.2a). This difference indicates that larger rainfall events tend to have greater stratiform regions as compared to smaller rain events. The relative contribution of isolated rain is also substantially less in the upper tercile of rainfall events (Fig. 4.2a) compared to in

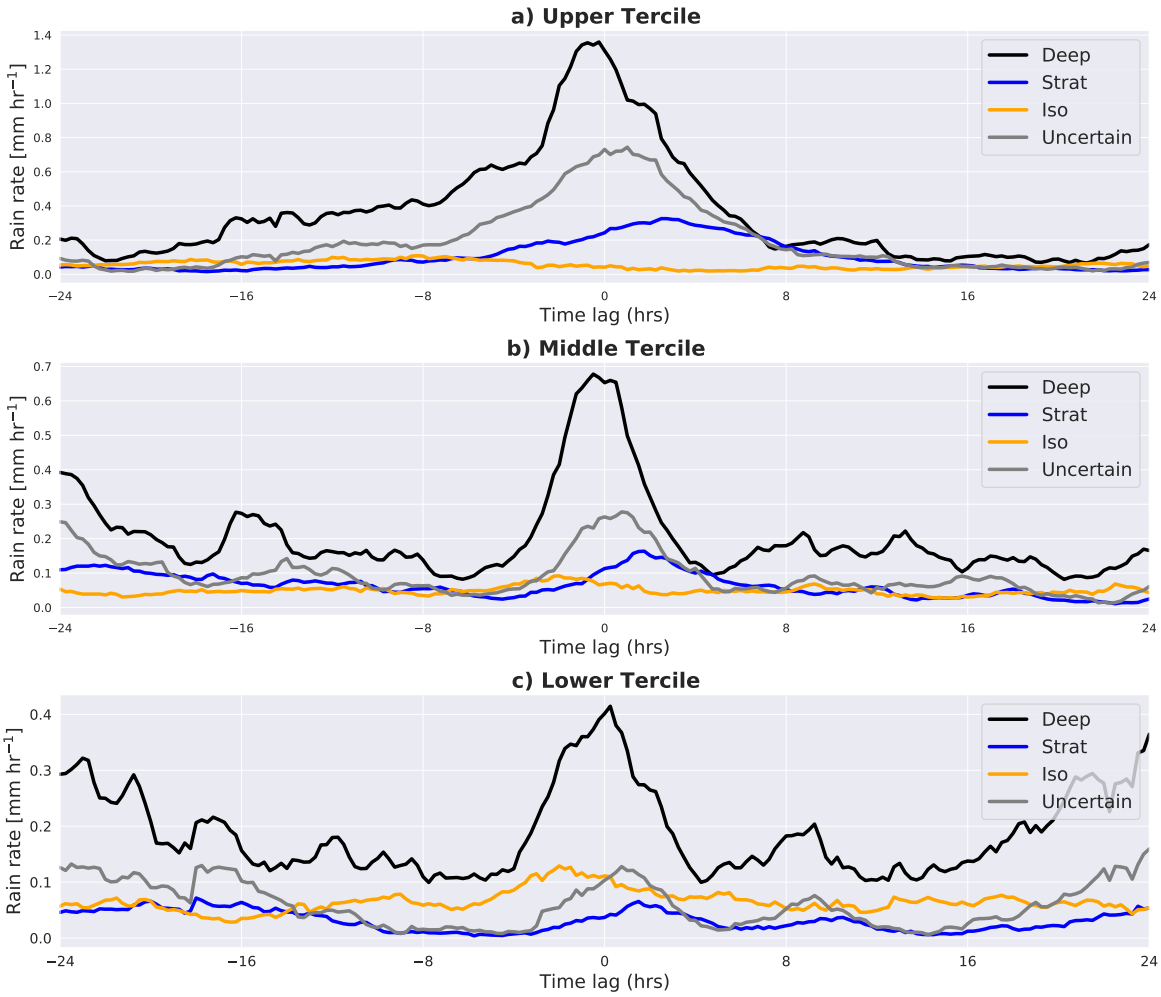


Figure 4.2: Rain rate composites for the lower tercile (a), middle tercile (b), and upper tercile (c). Each rain rate tercile composite is separated into contributions from deep rain clusters (black line), stratiform rain (blue line), isolated rain clusters (yellow), and uncertain (grey line) as determined by the Powell et al. 2016.

the lowest tercile (Fig. 4.2c). These results suggest upper tercile events consist of predominantly deep and stratiform rain clusters, while isolated rain clusters play a larger role in lower tercile rain events.

It is also important to note the difference in timing and progression of peak rainfall from each rain type in Fig. 4.2. Within all three terciles, deep convective rain typically peaks at or just prior to τ = 0hr. In contrast, stratiform rain typically peaks a few hours after τ = 0hrs. Comparing the upper tercile of events (Fig. 4.2a) to the lowest tercile (Fig. 4.2c) reveals that the time between peak in deep convective and stratiform rainfall decreases as the intensity and duration of the rainfall event decreases. This implies that upper tercile events generate larger and more organized stratiform cloud regions compared to lower tercile events. Fig. 4.2 further captures how rain from isolated clusters peaks a couple hours (e.g. τ = -2 to -3hrs) prior to deep convective rainfall peak, with the greatest amount contributing to lower and middle tercile events. These results show cloud organization evolves from isolated rain clusters to a mixture of deep and stratiform during rainfall events, supporting the proposed 3 stage process of cloud organization discussed in chapter 3.

4.1.2 Cloud Organization in Tercile Separated Rainfall Events

Following the analysis methods of Section 4.1.1, cloud organization indices from section 2.2 are applied to the rainfall events within each tercile. Organization indices are then composited within each tercile and lagged with the domain mean rain rate from τ=-24hrs to τ=+24hrs. The resulting time lag analyses capture how all rain clusters (Fig. 4.3) and deep convective rain clusters (Fig. 4.4) evolve leading up to and following peak rain rate within the most intense (upper tercile), least intense (lower tercile), and in-between (middle tercile) strength and duration rainfall events.

Initial inspection reveals there are several differences between how clouds organize within the upper tercile versus the lower tercile. For example, at τ = 0hrs SCAI is minimum in the upper tercile (Fig. 4.3c, black line), while it is maximum in the lower tercile (Fig. 4.3c, dark blue line). As previously discussed, SCAI strongly depends on the number N of clusters, increasing when there there are more clusters and decreasing when there are fewer clusters. Therefore it can be inferred that in upper tercile (i.e. most intense) events where SCAI is small, less N rain clusters are present at peak rainfall.

This is indeed true in Figure 4.5, which depicts the evolution of an upper tercile rainfall event that occurred from 15-16th of October, 2011. In this particular rainfall event at τ = 0hrs (Fig. 4.5, row 2), there are few separate rain clusters present as reflected in the low SCAI value from (Fig. 4.3c). However, the clusters which are present are quite large and cover most of the radar domain area. By comparison, the rain clusters that occur in lower tercile events, such as in figure 4.6 of an event that occurred November 16th, 2011, are typically much smaller in size. This reasserts the notion that while SCAI can give accurate information about the number of clusters present, it does not consider information about the size distribution of clusters present.

Further differences can be distinguished between how rain clusters organize within upper tercile and lower tercile rainfall events. For example, upper tercile rain clusters cover more radar domain area at τ = 0hrs, while lower tercile rain clusters cover less domain area. This is apparent through MICA in figure 4.3, which is smaller in upper tercile events and larger in lower tercile events. MICA decreases as the clear area fraction decreases, therefore the smaller MICA value reflects a greater coverage of rain clusters within the domain. This is clearly visible in the upper tercile event (Fig. 4.5)

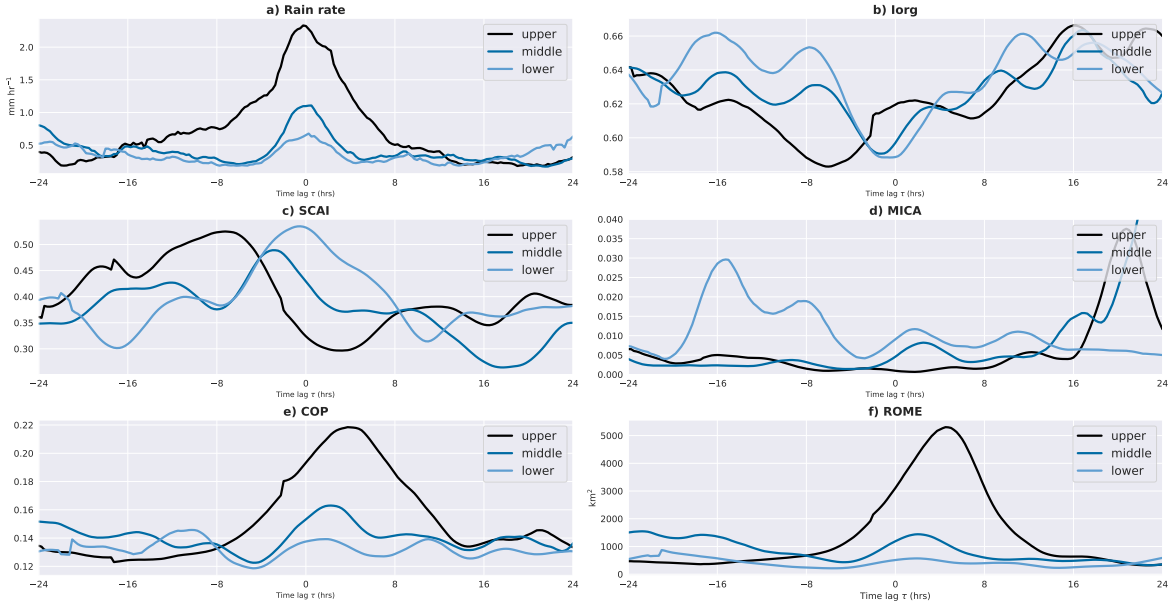


Figure 4.3: Composites of domain mean rain rate (mm/hr) (a) and I_{org}, SCAI (c), MICA (d), COP (e), and ROME (f) organization indices for all rain clusters in lower (light blue), middle (blue), and upper (black) tercile separated rainfall events. Each tercile is lagged with the domain mean rain rate from τ=-24hrs to τ=+24hrs.

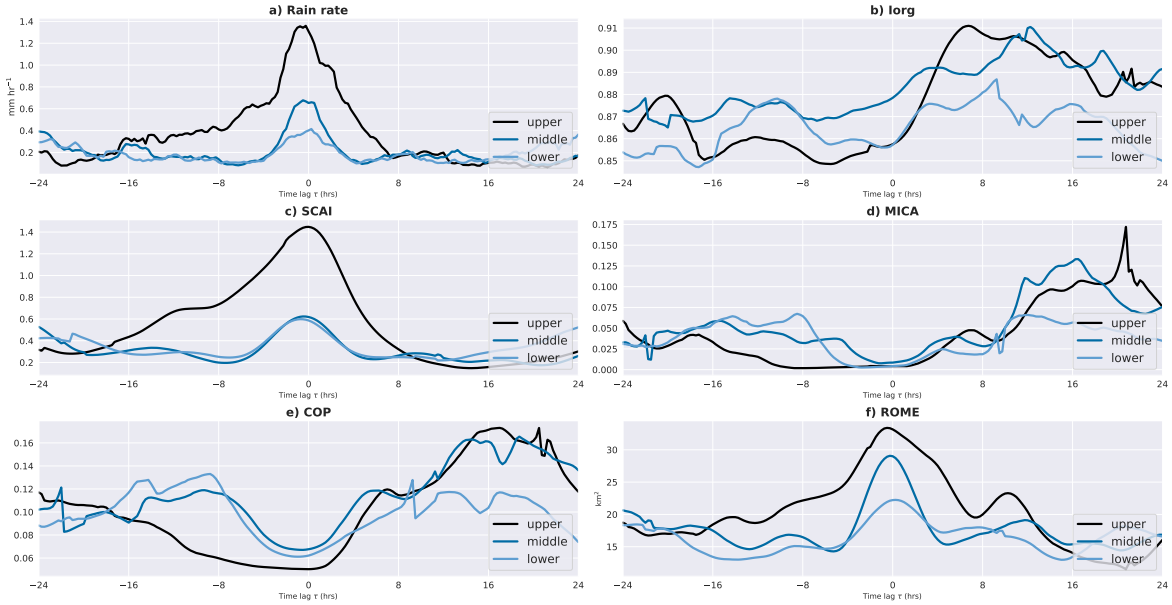


Figure 4.4: Composites of domain mean rain rate (mm/hr) (a) and I_{org}, SCAI (c), MICA (d), COP (e), and ROME (f) organization indices for deep convective rain clusters in lower (light blue), middle (blue), and upper (black) tercile separated rainfall events. Terciles are lagged with domain mean rain rate from τ=-24hrs to τ=+24hrs.

where much of the domain is covered by rain clusters, compared to the lower tercile event (Fig. 4.6), which has comparatively less rain cluster domain coverage.

The difference in domain coverage is also evident in ROME and COP (Fig. 4.3 e,f) which reflect a larger relative size and proximity of rain clusters with greater index values in upper tercile events and smaller cluster sizes with smaller values in lower tercile events. I_{org} reflects upper tercile rain clusters being more non-randomly distributed compared to lower tercile rain clusters at τ = 0hrs. Looking at the upper tercile event (Fig. 4.5), it is easy to discern the non-random distribution between τ =-8hrs and τ = 0hrs given the large increase in domain coverage by rain clusters leading up to peak rainfall. Within the lower tercile event however (Fig. 4.6), the evolution of rain clusters towards an increasingly more non-random distribution does not occur until τ = 0hrs and τ = +4hrs. This is likely explained by the increase in number of rain clusters from τ = -4hrs to τ = 0hrs before decreasing again from τ = 0hrs to τ = 4hrs. It is curious to note that regardless of intensity and duration, rain clusters become increasingly non-randomly distributed after peak rainfall. This implies that rain clusters decay non-randomly such that isolated rain clusters are the first to disappear, while larger clusters such as stratiform and deep convective clusters remain and take more time to decay. While I_{org} is limited in its ability to discern information about the spread in rain cluster size between upper and lower tercile events, its consistent increasing behavior following peak rainfall makes it therefore useful to help identify the particular stage of organization a rainfall event is in.

Deep convective rain clusters exhibit a different evolution compared to all rain clusters within upper and lower terciles. For instance, SCAI maximizes at τ = 0hr for deep convective rain clusters in all terciles (Fig. 4.4c). This contrasts with the behavior of SCAI in the upper tercile of all rain clusters at τ = 0hr (Fig. 4.3c), which

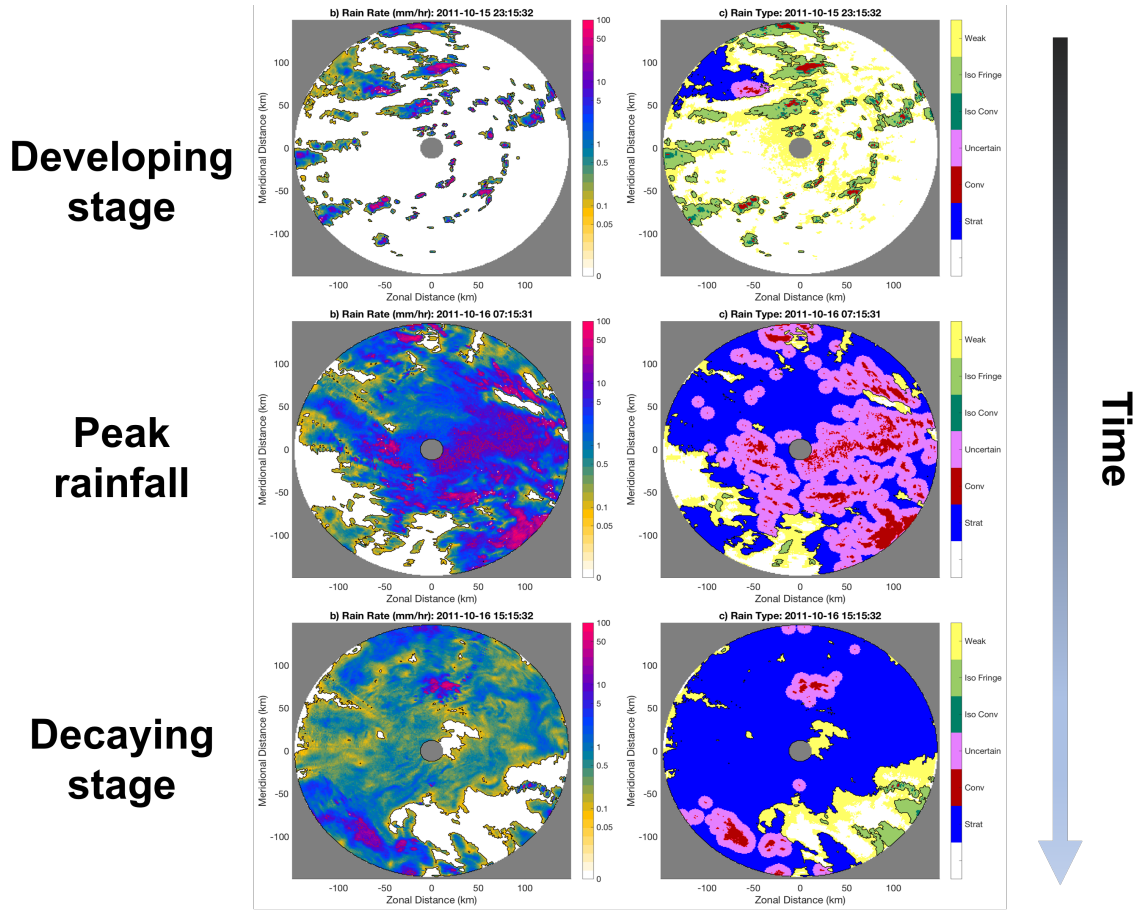


Figure 4.5: S-PolKa radar estimated rain rate (mm/hr) (left column) and rain type separation (right column) for an upper tercile rainfall event that occurred October 16, 2011. Scans show the progression of cloud organization from 8hrs prior to peak rain rate (row 1), time of peak rain rate (row 2), and 8hrs following peak rain rate (row 3).

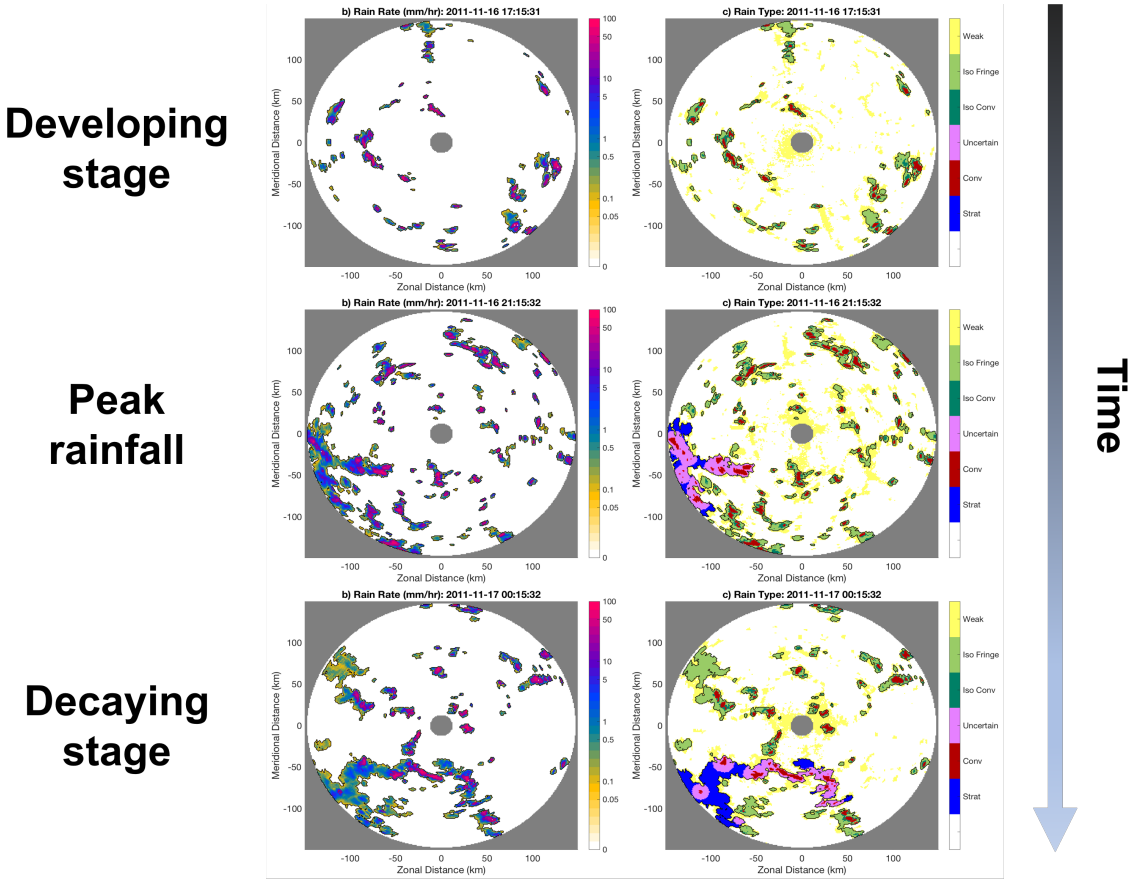


Figure 4.6: S-PolKa radar estimated rain rate (mm/hr) (left column) and rain type separation (right column) for a lower tercile rainfall event that occurred November 16, 2011. Scans show the progression of cloud organization from 4hrs prior to peak rain rate (row 1), time of peak rain rate (row 2), and 4hrs following peak rain rate (row 3).

is a minimum after peak rainfall. The maximum in SCAI for deep convection (Fig. 4.4c) signals that the number N of deep rain clusters are greatest at peak rainfall, before decreasing over time alongside rain rate. This result suggests deep convective clusters are the primary convective type present at peak rainfall (τ = 0hr). This is indeed observed in the rightmost panels of the upper tercile event (Fig. 4.5) and lower tercile event (Fig. 4.6). In both cases, deep convective rain clusters (red shadings) are greatest at τ = 0hr, with visibly less deep rain clusters present in the hours leading up to and following peak rainfall.

Other differences are apparent between the evolution of deep rain clusters compared to all rain clusters. For instance, COP is a local minimum at τ = 0hrs across all terciles for deep rain clusters (Fig. 4.4e), decreasing prior to peak rainfall and increasing after peak rain. The decrease in COP leading up to peak rain rate reflects the increase in proximity of deep rain clusters as more form leading up to τ = 0hrs. The subsequent increase in COP after peak rainfall is then explained by the distance once again increasing between deep rain clusters. These transitions are noticeable in both the upper tercile event (Fig. 4.5) and lower tercile event (Fig. 4.6), although not as clearly in the lower tercile events. Another difference is how the ROME organization index peaks at τ = 0hrs for deep convective rain clusters (Fig. 4.4f) compared to all rain clusters (Fig. 4.3f) after peak rainfall. This further supports the finding that deep rain clusters are dominant at peak rainfall, and is visible comparing deep rain clusters in figures 4.5 and 4.6 to all rain clusters (all colors combined).

Analyzing how organization indices evolve within upper, middle, and lower tercile events reveals the differences in the extent to which clouds organize in intense and longer duration rainfall events compared to weaker and shorter duration rainfall events. As demonstrated by figure 4.3a, the most intense or enhanced rain events (i.e. upper

tercile) typically persist on the order of 2-days and evolve into MCSs or systems of enhanced convection, while less intense events last on the order of <1 day and never fully realize the second stage of typical cloud organization proposed in the previous chapter (Fig. 3.4). For intense rainfall events, rain clusters quickly evolve in the developing stage from isolated convective clusters to larger, aggregated systems characterized by predominantly deep convective rain clusters and surrounding stratiform convection. At this stage, deep convection contributes to the majority of the total rain rate. Transitioning from this second stage to the third decaying phase, rainfall decreases alongside deep rain clusters that are replaced by larger regions of stratiform, with remaining deep convection becoming increasingly non-randomly distributed. Weaker rain events (i.e. middle and lower terciles) exhibit a much different evolution of organization in comparison. Most profoundly, weaker events seem to never quite reach the second stage of organization that more intense ones do. Rather, weaker rainfall events are considerably "dis-aggregated" at rainfall peak and consist of primarily isolated convection with no to limited MCS development. A larger contributor of rainfall to the peak rainrate is also from isolated clusters in comparison to deep convective rain clusters. As weak rain events reach their respective decaying stage, they fail to develop large regions of clustered stratiform or occupy much of the radar domain.

Indeed, these findings challenge how cloud organization is defined. Is it best defined by a number of different parameters and spatial characteristics? Or is it rather a linear process that continuously evolves depending on the right conditions? In the next section, potential mechanisms will be discussed that drive tropical rain events, as well as proposed differences that may determine whether topical rainfall events are weaker or more intense. Concluding this section, it has been shown through cloud organization indices that there are large differences between the evolution of stronger and longer duration rainfall events and weaker and shorter rainfall events.

Chapter 5

Summary and Conclusions

The objective of this study was to understand how cloud organization evolves within observed rainfall events during the DYNAMO/AMIE field campaign. It was first shown that five cloud organization indices disagree on the strength and evolution of organization in rain clusters and deep rain clusters leading up to and following maximum rain rate. The inconsistencies between cloud organization indices are explained by their dependence on different variables and parameters in their calculation. Due to the discrepancies between cloud organization indices, the evolution of properties associated with cloud organization indices were examined including number, distance, proximity, and size of clusters. Analyzing these properties revealed that rain clusters and deep rain clusters organize in three typical phases - a developmental phase, a sustained phase, and a decaying phase.

Within the developmental phase, rain clusters are greatest in number and are least aggregated while deep rain clusters are fewer in number and more non-randomly distributed. As organization evolves to the sustained phase, the number of non-deep rain clusters decreases. Rain clusters that remain in this phase merge closer together and grow in mean size. Deep rain clusters also increase in number and size during this phase. Finally, as evolution progresses to the decaying phase the number of rain clusters and deep convective rain clusters decreases, with remaining clouds clustering preferentially near other convection.

We also found characteristic differences between the evolution of cloud organization in the most intense, longest duration rainfall events and weaker, shorter duration rainfall events. Within the most intense events, rain clusters exhibit the greatest degree of aggregation, largest mean size, non-randomness, and clustering during the second phase immediately after peak rainfall. By comparison, the weakest rainfall events exhibit high dis-aggregation and randomness of rain clusters at rainfall peak. The weakest rainfall events never fully reach the organization stages that the most intense events go through. For instance, the weakest rainfall events do not evolve from the developing phase to the sustained phase of organization in figure 3.4. This suggests that cloud organization and evolution in rainfall events is a process of upscale growth that occurs under the right conditions and environmental setup. Maximum spatial non-randomness of clusters in the decaying phase of rainfall events further supports this argument and contradicts the theory that organization leads to upscale growth of organized convection (Sakaeda and Torri 2022).

Several physical processes have been observed to drive development and evolution of tropical maritime convective systems at different stages. Boundary layer (BL) cold pools have been previously found to promote growth of new convective updrafts near existing clusters in the developmental phase (Cheng et al. 2020). The same study also discussed the importance of lower free-tropospheric wind shear in constraining convection to form preferentially in moister regions via entrainment of environmental air into updrafts. As convection evolves into an enhanced or sustained phase, these processes become less influential. Instead, a mesoscale circulation driven by convective region diabatic heating and stratiform rain evaporation enhances BL convergence and helps to sustain the developed convective systems.

Considering the many different processes responsible for sustaining convective organization, what then stops weaker rainfall events such as Fig. 4.6 from developing into

stronger, longer sustained events like that in Fig. 4.5? One potential mechanism could be large-scale forcing from the MJO, which is known to provide more environmental moisture during its enhanced phase. Other plausible mechanisms include the weakening of lower tropospheric moisture variations Cheng et al. (2020) or a maximization in vertical wind shear Sakaeda and Torri (2022), which could each act to weaken the mesoscale circulation. How and to what extent each of these mechanisms influence the development of tropical convection in the context of large-scale forcings still remains an unknown however, and would be particularly useful to investigate in future work.

Reference List

Biagioli, G., and A. M. Tompkins, 2023: Measuring convective organization. *Journal of the Atmospheric Sciences*, **80 (12)**, 2769 – 2789, https://doi.org/10.1175/JAS-D-23-0103.1.

Cheng, W.-Y., D. Kim, and A. Rowe, 2018: Objective quantification of convective clustering observed during the amie/dynamo two-day rain episodes. *Journal of Geophysical Research: Atmospheres*, **123**, 10,361–10,378, https://doi.org/10.1029/2018JD028497.

Cheng, W. Y., D. Kim, A. Rowe, Y. Moon, and S. Wang, 2020: Mechanisms of convective clustering during a 2-day rain event in amie/dynamo. *Journal of Advances in Modeling Earth Systems*, **12**, https://doi.org/10.1029/2019MS001907.

Hartmann, D. L., H. H. Hendon, and R. A. Houze, 1984: Some implications of the mesoscale circulations in tropical cloud clusters for large-scale dynamics and climate. *Journal of Atmospheric Sciences*, **41 (1)**, 113 – 121, https://doi.org/10.1175/1520-0469(1984)041%3C0113:SIOTMC%3E2.0.CO;2.

Kadoya, T., and H. Masunaga, 2018: New observational metrics of convective self-aggregation: Methodology and a case study. *Journal of the Meteorological Society of Japan. Ser. II*, **96 (6)**, 535–548, https://doi.org/10.2151/jmsj.2018-054.

Mapes, B., and R. Neale, 2011: Parameterizing convective organization to escape the entrainment dilemma. *Journal of Advances in Modeling Earth Systems*, **3 (2)**, https://doi.org/https://doi.org/10.1029/2011MS000042.

Nesbitt, S. W., R. Cifelli, and S. A. Rutledge, 2006: Storm morphology and rainfall characteristics of trmm precipitation features. *Monthly Weather Review*, **134 (10)**, 2702 – 2721, https://doi.org/10.1175/MWR3200.1.

Powell, S. W., R. A. Houze, and S. R. Brodzik, 2016: Rainfall-type categorization of radar echoes using polar coordinate reflectivity data. *Journal of Atmospheric and Oceanic Technology*, **33 (3)**, 523 – 538, https://doi.org/10.1175/JTECH-D-15-0135.1.

Retsch, M. H., C. Jakob, and M. Singh, 2020: Assessing convective organization in tropical radar observations. *Journal of Geophysical Research: Atmospheres*, **125 (7)**, e2019JD031 801, https://doi.org/10.1029/2019JD031801.

Rutledge, S., P. F. Hein, B. Dolan, S. W. Powell, and S. R. Brodzik, 2012: Ncar s-polka radar data: Dynamo legacy data products.

Sakaeda, N., and G. Torri, 2022: The behaviors of intraseasonal cloud organization during dynamo/amie. *Journal of Geophysical Research: Atmospheres*, **127**, https://doi.org/10.1029/2021JD035749.

Stein, T. H. M., C. E. Holloway, I. Tobin, and S. Bony, 2017: Observed relationships between cloud vertical structure and convective aggregation over tropical ocean. *Journal of Climate*, **30 (6)**, 2187 – 2207, https://doi.org/10.1175/JCLI-D-16-0125.1.

Thompson, E. J., S. A. Rutledge, B. Dolan, M. Thurai, and V. Chandrasekar, 2018: Dual-polarization radar rainfall estimation over tropical oceans. *Journal of Applied Meteorology and Climatology*, **57 (3)**, 755 – 775, https://doi.org/10.1175/JAMC-D-17-0160.1.

Tobin, I., S. Bony, and R. Roca, 2012: Observational evidence for relationships between the degree of aggregation of deep convection, water vapor, surface fluxes, and radiation. *Journal of Climate*, **25**, 6885–6904, https://doi.org/10.1175/JCLI-D-11-00258.1.

Tompkins, A. M., and A. G. Semie, 2017: Organization of tropical convection in low vertical wind shears: Role of updraft entrainment. *Journal of Advances in Modeling Earth Systems*, **9 (2)**, 1046–1068, https://doi.org/10.1002/2016MS000802.

White, B. A., A. M. Buchanan, C. E. Birch, P. Stier, and K. J. Pearson, 2018: Quantifying the effects of horizontal grid length and parameterized convection on the degree of convective organization using a metric of the potential for convective interaction. *Journal of the Atmospheric Sciences*, **75 (2)**, 425 – 450, https://doi.org/10.1175/JAS-D-16-0307.1.

Wing, A. A., and K. A. Emanuel, 2014: Physical mechanisms controlling self-aggregation of convection in idealized numerical modeling simulations. *Journal of Advances in Modeling Earth Systems*, **6 (1)**, 59–74, https://doi.org/10.1002/2013MS000269.

Yoneyama, K., C. Zhang, and C. N. Long, 2013: Tracking pulses of the madden–julian oscillation. *Bulletin of the American Meteorological Society*, **94 (12)**, 1871 – 1891, https://doi.org/10.1175/BAMS-D-12-00157.1.

Zuluaga, M. D., and R. A. Houze, 2013: Evolution of the population of precipitating convective systems over the equatorial indian ocean in active phases of the madden-julian oscillation. *Journal of the Atmospheric Sciences*, **70**, 2713–2725, https://doi.org/10.1175/JAS-D-12-0311.1.